Nov 5th, 12:00 AM - 12:00 AM

Development of a New Beam-Column Design Method for Cold-Formed Steel Lipped Channel Members

Shahabeddin Torabian

Baofeng Zheng

Benjamin W. Schafer

Twenty-Second International Specialty Conference on Cold-Formed Steel Structures
St. Louis, Missouri, USA, November 5 & 6, 2014

Development of a new beam-column design method for cold-formed steel lipped channel members

Shahabeddin Torabian[1], Baofeng Zheng[2], Benjamin W. Schafer[3]

Abstract

The structural strength of cold-formed steel lipped channels under combined axial force and biaxial bending moments has been predicted by geometric and material nonlinear collapse analyses performed in ABAQUS and compared to both current, and a newly proposed, beam-column design method. The ABAQUS analyses utilizes a validated modeling protocol calibrated against previous testing by the authors, and including residual stresses and strains, and geometric imperfections; as well as, appropriate cross-section dimensions, member length, and boundary conditions. A total of 75 different lipped channel cross-sections have been selected and the capacity of the beam-column member has been examined under 127 combinations of actions in the P-M_1-M_2 space (axial load, P, and major-axis, M_1, and minor-axis, M_2, bending moments). The results have been used to evaluate the current beam-column design method and validate a new Direct Strength Method (DSM) approach for cold-formed steel beam-columns. The newly proposed method provides means to incorporate more realistic stability analyses of cross-sections under the applied actions, where the current design methods include only a linear prediction of the combined actions using "column strength" and "beam strength" as anchor points. Correspondingly, the reliability of both current and newly proposed methods has been evaluated. The newly proposed extensions to the Direct Strength Method show a potential to realize a sizeable strength increase in many situations, and follow the overall trends in the data (P-M_1-M_2 surface) well; however, additional advancement is needed to realize the complete benefits predicted in the finite element models.

[1] Assistant Research Scientist, Johns Hopkins University, Baltimore, MD, 21218, USA. (torabian@jhu.edu)
School of Civil Engineering, College of Engineering, University of Tehran. (torabian@ut.ac.ir)
[2] PhD candidate, Southeast University, Nanjing, 210096, China. (bzheng3@jhu.edu) formerly Visiting Student Scholar, Johns Hopkins University, Baltimore, MD, 21218. USA.
[3] Professor and Chair, Johns Hopkins University, Baltimore, MD, 21218, USA. (schafer@jhu.edu)

Introduction

The Direct Strength Method (DSM) is a recently developed design method for cold-formed steel structural members that explicitly takes cross-section stability into account through enabling the implementation of advanced computational analyses, such as the finite strip method, to determine the elastic buckling loads of the member in local, distortional and/or global modes of failure, including interactions. The elastic buckling loads drive a series of design strength equations to determine both axial and bending moment capacity of cold-formed structural members, e.g. lipped channels and Zee sections. Current design codes such as the North American Specification of the American Iron and Steel Institute (AISI-S100, 2012) and the Australian/New Zealand Standard (AZ/NZS) for cold-formed steel structures (AS/NZS 2005) formally provide the traditional Effective Width Method (EWM), and the Direct Strength Method (DSM) (AISI-S100, 2012; Standards Australia, 2005). See Schafer (2008) for a complete review..

Although extensive efforts have been devoted to estimating the capacity of cold-formed steel members under pure axial or flexural actions (Hancock, 2003; Macdonald, Heiyantuduwa, & Rhodes, 2008; Rondal, 2000; Schafer, 2008; Young, 2008), the design of structural members under explicit combined actions has seen less study in both EWM and DSM (Kalyanaraman & Jayabalan, 1994; Loh, 1985; Miller & Pekoz, 1994; Pekoz, 1986; Peterman, 2012; Shifferaw, 2010; Yiu & Pekoz, 2000). The combined effect of the actions on the member is taken into account in the latest design specifications, e.g. in AISI-S100-12, through a simple linear combination of the isolated pure axial or flexural design previously determined using EWM or DSM. Therefore, the current cold-formed steel beam-column design methods ignore any nonlinear interaction in the strength between axial load and bending.

In this paper, comprehensive parametric geometric and material nonlinear collapse analyses, particularly on lipped channels, have been used to evaluate the structural reliability of both current and newly proposed beam-column design methods. The newly proposed method includes more realistic stability analyses of cross-sections under the applied actions. The analyses follow a modeling protocol verified against relevant experimental results. The results show the potential to improve the current beam-column design method. The newly proposed beam-column DSM has the potential to realize much of the strength increase in many situations, and follows the overall trends in the data (P-M_1-M_2 strength surface) well; however, additional advancement is needed to realize the complete benefits predicted in the finite element models. The following sections include a brief description of the new beam-column DSM,

including formal definition of the P-M_1-M_2 space, elastic stability of the beam-columns under combined actions and elastic buckling surface in P-M_1-M_2 space, verified modeling protocols for parametric analyses, cross-section and length selection criteria for parametric analyses, and the analyses results and the reliability analysis and discussions.

The results presented herein are a part of an ongoing comprehensive study developing a new explicit DSM prediction for cold-formed steel beam-columns. The larger effort includes additional tests and numerical analyses on cold-formed steel Zee sections and further refinement of the DSM formulation.

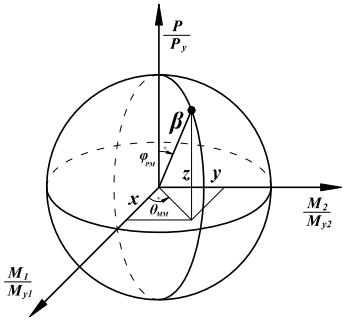

Figure 1 Normalized P-M_1-M_2 Space

Direct strength prediction for Beam-Columns (DSM Beam-Columns)

Normalized P-M_1-M_2 Space

The use of a generalized coordinate system is important in the development of the new design method. The P-M_1-M_2 space is implemented to define the state of the applied combined actions including bi-axial bending moments (M_1, M_2) and axial force (P) with respect to the corresponding yield strength, as follows (also see Figure 1),

$$x = \frac{M_1}{M_{y1}}, y = \frac{M_2}{M_{y2}}, z = \frac{P}{P_y} \qquad (1)$$

where, M_1 and M_2 are two orthogonal (principal) axes of the cross section and the denominators (subscript y) are the corresponding yield moments (force).

Points in the normalized P-M_1-M_2 space are defined by an azimuth angle, θ_{MM}, an elevation angle, ϕ_{PM} , and a radial length β :

$$\theta = tan^{-1}(y/x),\ \phi_{MM} = cos^{-1}(z/\beta),\ \beta = \sqrt{x^2 + y^2 + z^2} \qquad (2)$$

The normalized axial and bending moment strength of a member are just anchor points on the x, y, and z axes. Connecting all the points corresponding to the strength of a member associated with a particular θ_{MM} and ϕ_{PM} angles results in the strength surface of a member in 3D space.

New Beam-Column Direct Strength Method

The newly proposed beam-column DSM formulation is consistent with DSM for the design of beams and columns in AISI-S100-12. The method provides similar results for "beams" and "columns" at the anchor points, and more realistic strength prediction for the combined actions away from the anchors. Notably, anchor points are the points of either pure axial compression (ϕ_{PM}=0) or pure bending moments about one of the principal axes (ϕ_{PM}=90^o; θ_{MM}=0^o, 90^o, 180^o, 270^o). ϕ_{PM} determines how much a point is close to either "beam" or "column" conditions. All results are represented in β□ θ_{MM}□ ϕ_{PM} coordinate, where β shows how far a loading point can be pushed along the (θ_{MM}, ϕ_{PM}) line in P-M_1-M_2 space to reach a particular limit state such as elastic buckling, yield, or plastic limits.

Accordingly, for each loading condition such as (P_r, M_{r1}, M_{r2}) or ($\beta_{\square}$□ θ_{MM}□ ϕ_{PM}), the induced state of stress on the cross-section is used to determine elastic buckling loads such as local ($\beta_{\square\square L}$), distortional ($\beta_{\square\square D}$) and global ($\beta_{\square\square G}$) buckling loads. Moreover, the stress distribution along the (θ_{MM}, ϕ_{PM}) line is used to determine β corresponding to the first yielding of the cross-section, $\beta_{y.}$ Calculation of the plastic strength of the section, $\beta_{p,}$ is not as trivial as the first yield capacity of the cross-section. A fully plastic distribution of stress on the cross-section can result in two different axes for the loading axis and the neutral axis of the cross-section. This phenomenon provides difficulties in finding of plastic surface of the sections, which are not within the scope of this paper.

In all buckling modes, the design equations are a function of the associated slenderness consistent with DSM "beam" and "column" design equations. The proposed method can incorporate inelastic reserve, effects of holes in the design, and design under tension force and bending moments. The effects of holes and tension are not discussed herein.

Global Buckling

The nominal capacity of a beam-column in global buckling, $\beta_{\square\square}$, is calculated as a function of global slenderness λ_G, defined as follows:

$$\lambda_G = \sqrt{\beta_y / \beta_{crG}} \tag{3}$$

Since inelastic reserve (capacity greater than first yield) is available only in bending, the nominal capacity, $\beta_{\square\square}$, is considered to be a function of the nominal capacity in axial compression, $\beta_{\square\square P}$, and the nominal flexural capacity, $\beta_{\square\square M}$, including inelastic reserve, as follows.

$$\beta_{nG} = \beta_{nGP} + (\beta_{nGM} - \beta_{nGP}) \sin\phi_{PM} \tag{4}$$

The proposed DSM equations for global buckling under combined axial load and bending are presented in the following,

For compression: $0 \le \phi_{PM} < \pi/2$

$$\beta_{nGP} = 0.658^{\lambda_G^2} \beta_y \quad \text{for } \lambda_G \le 1.5 \tag{5}$$

$$\beta_{nGP} = 0.877 \beta_{crG} \quad \text{for } \lambda_G > 1.5 \tag{6}$$

For bending: $0 < \phi_{PM} < \pi$, $0 \le \theta_{MM} \le 2\pi$

$$\beta_{nGM} = \beta_p \quad \text{for } \lambda_G \le 0.23 \tag{7}$$

$$\beta_{nGM} = \beta_p - (\beta_p - \beta_y)\frac{\lambda_G - 0.23}{0.37} \quad \text{for } 0.23 < \lambda_G < 0.60 \tag{8}$$

$$\beta_{nGM} = \beta_y \text{ (no inelastic reserve)} \quad \text{for } \lambda_G \le 0.60 \tag{9}$$

$$\beta_{nGM} = \frac{10}{9}\beta_y\left(1 - \frac{10\beta_y}{36\beta_{crG}}\right) \quad \text{for } 0.60 \le \lambda_G \le 1.34 \tag{10}$$

$$\beta_{nGM} = \beta_{crG} \quad \text{for } \lambda_G > 1.34 \tag{11}$$

Local Buckling

Consistent with the DSM method in AISI-S100-12, local-global interaction is adopted in the proposed beam-column DSM. The nominal capacity of beam-columns in local buckling, $\beta_{\square L}$, can be determined here as a function of local slenderness λ_L, defined as follows:

$$\lambda_L = \sqrt{\frac{\beta_{nG}}{\beta_{crL}}} \text{ for } \beta_{nG} \le \beta_y \; ; \; \lambda_L = \sqrt{\frac{\beta_y}{\beta_{crL}}} \text{ for } \beta_{nG} > \beta_y \tag{12}$$

As local buckling equations for "beams" and "columns" are of the same format in DSM, the new equations for beam-column DSM also provide a consistent set of equations including local-global interaction and inelastic reserve as follows,

for $\lambda_L \le 0.776$

Inelastic reserve capacity for symmetric members or when the first yield is in compression ($\beta_{nG} > \beta_y$):

$$\beta_{nL} = \beta_y + \left(1 - 1/C_{yL}^2\right)\left(\beta_p - \beta_y\right),\ C_{yL} = \sqrt{0.776/\lambda_L} \le 3 \quad (13)$$

Inelastic reserve capacity the first yield is in tension, conservative approach ($\beta_{nG} > \beta_y$):

$$\beta_{nL} = \beta_y + \left(1 - 1/C_{yL}^2\right)\left(\beta_p - \beta_y\right) \le \beta_{yt3}$$

$$\beta_{yt3} = \beta_y + 8/9\left(\beta_p - \beta_y\right) \quad (14)$$

Ignoring inelastic reserve capacity:

$$\beta_{nL} = \beta_y\ ,\ \beta_{nG} > \beta_y$$

$$\beta_{nL} = \beta_{nG}\ ,\ \beta_{nG} \le \beta_y \quad (15)$$

for $\lambda_L > 0.776$

$$\beta_{nL} = \left[1 - 0.15\left(\frac{\beta_{crL}}{\beta_{nG}}\right)^{0.4}\right]\left(\frac{\beta_{crL}}{\beta_{nG}}\right)^{0.4} \beta_{nG} \text{ for } \beta_{nG} \le \beta_y$$

$$\beta_{nL} = \left[1 - 0.15\left(\frac{\beta_{crL}}{\beta_y}\right)^{0.4}\right]\left(\frac{\beta_{crL}}{\beta_y}\right)^{0.4} \beta_y \text{ for } \beta_{nG} \ge \beta_y$$

Distortional Buckling

Consistent with the DSM method in AISI-S100-12, distortional-global interaction is ignored in the proposed beam-column DSM. The nominal capacity of beam-columns in distortional buckling, $\beta_{\square D}$, is determined here as a function of distortional slenderness λ_D calculated as follows,

$$\lambda_D = \sqrt{\frac{\beta_y}{\beta_{crd}}} \quad (16)$$

As distortional buckling equations for "beams" and "columns" are almost consistent in DSM, the new equations for beam-column DSM provides a set of equations with the slenderness limits dependent on ϕ_{PM}, as follows,

for $\lambda_D \le 0.561 + 0.112 \sin\phi_{PM}$

Inelastic reserve capacity for symmetric members or when the first yield is in compression:

$$\beta_{nD} = \beta_y + \left(1 - 1/C_{yD}^2\right)\left(\beta_p - \beta_y\right)$$

$$C_{yD} = \sqrt{\left(0.561 + 0.112\sin\phi_{PM}\right)/\lambda_{crD}} \le 3 \qquad (17)$$

Inelastic reserve capacity the first yield is in tension, conservative approach ($\beta_{nG} > \beta_y$):

$$\beta_{nD} = \beta_y + \left(1 - 1/C_{yD}^2\right)\left(\beta_p - \beta_y\right) \le \beta_{yt3}$$

$$\beta_{yt3} = \beta_y + 8/9\left(\beta_p - \beta_y\right) \qquad (18)$$

Ignoring inelastic reserve capacity:

$$\beta_{nD} = \beta_y \qquad (19)$$

for $\lambda_D > 0.561 + 0.112 \sin\phi_{PM}$

$$\beta_{nD} = \left(1 - c_1\left(\frac{\beta_{crd}}{\beta_y}\right)^{c_2}\right)\left(\frac{\beta_{crd}}{\beta_y}\right)^{c_2}\beta_y$$

$$c_1 = 0.25 - 0.03\sin\phi_{PM},\ c_2 = 0.6 - 0.1\sin\phi_{PM} \qquad (20)$$

Design Check

The nominal capacity of the beam-column at the particular direction (θ_{MM}, ϕ_{PM}) in P-M_1-M_2 can be calculated as follows,

$$\beta_n = min\left(\beta_{nL}, \beta_{nD}, \beta_{nG}\right) \qquad (21)$$

For design purposes, the capacity of the member including the resistance factor ϕ □□□LRFD method or safety factor Ω □□ allowable stress design method should satisfy the following design equations,

$$\beta_r \le \phi\beta_n \ or\ \beta_r \le \beta_n/\Omega \qquad (22)$$

Elastic buckling analysis

The proposed beam-column DSM requires elastic buckling analysis under any required action. All elastic critical surfaces are determined from stability analysis using CUFSM 4.06 (Schafer & Adany, 2006) assuming the actual stress distribution. Specifically, each desired point on the P-M_1-M_2 surface is on a line

defined by azimuth (θ_{MM}) and elevation (ϕ_{PM}) angles. The elastic critical load factor for a particular point in the P-M_1-M_2 space is a normalized distance, β□□, between that point and the origin along the (θ_{MM}, ϕ_{PM}). The required actions (P_r, M_{r1}, M_{r2}) or (β□□θ_{MM}□ϕ_{PM}), induce a state of axial stress, f_r, on the cross-section as follows,

$$f_r = \frac{P_r}{A} + \frac{M_{r1} y_{cx}}{I_1} + \frac{M_{r2} x_{cx}}{I_2} \qquad (23)$$

where, I_1 and I_2 are principal moment of inertia, y_{cx} and x_{cx} are the distance to the centroidal principal axes, and A is the cross-sectional area. The cross-section stability analysis (using CUFSM) performed on f_r provides, buckling load factors (α_{crL}, α_{crD}, α_{crG}) for local (L), distortional (D), and global (G) buckling. These factors may be resolved back into the P-M_1-M_2 space simply as

$$\beta_{crL} = \alpha_{crL}\beta_r, \quad \beta_{crD} = \alpha_{crD}\beta_r, \quad \beta_{crG} = \alpha_{crG}\beta_r \qquad (24)$$

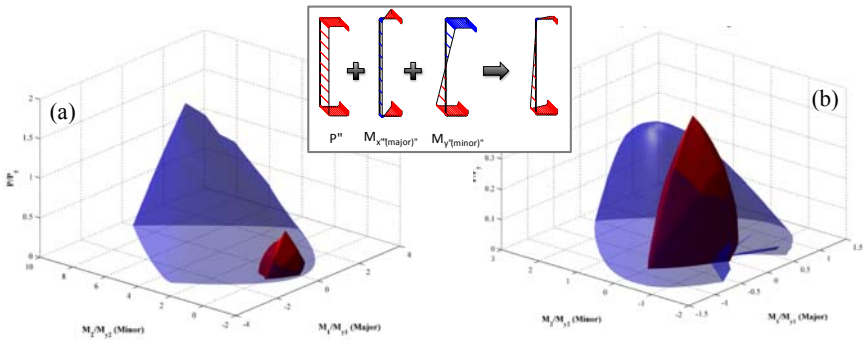

Figure 2 Elastic (blue) and nominal strength (red) surfaces under the combined actions-600S137-54 (L=12 inches): (a) local buckling; (b) distortional buckling

To automatically identify local and distortional buckling and avoid the problems of non-unique minima in conventional finite strip models, the newly proposed "*FSM@cFSM-L_{cr}*" method is used (Li & Schafer, 2010). "*FSM@cFSM-L_{cr}*" utilizes a straight-line cross-section and a constrained finite strip method (cFSM) analysis to determine buckling half-wave lengths (L_{cr}) for pure local and pure distortional buckling. These lengths are then used to uniquely identify the local and distortional buckling response and α_{crL}, and α_{crD}.

The elastic buckling load factors are used for predicting the design strength in accordance with the proposed formulas of the previous section. Figure 2 illustrates the elastic surfaces (in blue) for local (Figure 2a), and distortional buckling (Figure 2b) for an example cross-section. To enable comparison, the corresponded strength surface (in red) is also mapped into the space for a

600S137-54, L=12 inches. Strength may be less than, or greater than, the elastic buckling response, as dictated by the slenderness.

Numerical Modeling

The general-purpose finite element program ABAQUS is employed to perform a comprehensive parametric nonlinear collapse analyses on lipped channel beam-columns to evaluate the newly proposed beam-column DSM. The modeling protocols used in the parametric analyses are verified against experimental results as discussed in (Torabian, Zheng, & Schafer, 2014a, 2014b). The modeling protocols and assumptions in the analysis are briefly discussed in the following.

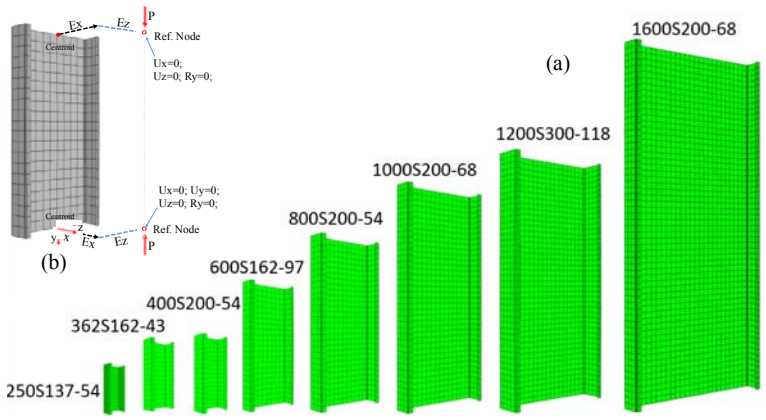

Figure 3 (a) Typical mesh topology (Maximum mesh size is 15mm); (b) Boundary conditions in the parametric study

Modeling protocols

Element, mesh properties and boundary conditions

The 9-node quadratic shell element, S9R5, is used as the computational element in the models. The maximum size of the element is assumed to be 15mm×15mm; the corners of the cross-section are meshed with 4 elements (transversally); the minimum number of transverse elements in the web, flange, and lip is considered to be 4, 2 and 2, respectively. The typical mesh topology for different size of specimens in the parametric study, and the assumed boundary conditions are shown in Figure 3a and Figure 3b, respectively.

Material model

Two nominal yield strengths of 33 ksi (228 MPa) and 50 ksi (345 MPa) are used in this study corresponding to the available strength of the products. An elastic-perfectly-plastic material model is adopted as a conservative model for the parametric analyses. The elastic Young's modulus and the Poisson's ratio are 29500 ksi (2.03×10^5 MPa) and 0.3, respectively. For the plastic behavior, von Mises yield criterion and associated flow are adopted.

Cold roll-forming effects

To include the cold roll-forming effects thirty-one through thickness integration points are required, which results in a large increase in computational effort. However, it has been shown that the cold roll-forming effect increases the member strength about 2% on average (Torabian et al., 2014a). Therefore, the cold roll-forming effect is ignored in the parametric study reported herein and no residual stress is introduced into the finite element models. This assumption can lead to make the parametric study modeling protocol modestly biased (conservatively) on the strength prediction (about -2%), which can be considered in the interpretation of the results.

Geometrical imperfections

To employ a generalized imperfection pattern in the parametric analysis, global, distortional, and local buckling modes are introduced into the finite element models consistent with the verification studies. As discussed in Torabian et al., (2014a) the finite element models with the "PGPDPL" imperfection pattern, which is defined as positive global, positive distortional, and positive local buckling shape pattern under uniform compression (see Figure 4 for the "positive" sign convention), provides a lower-bound prediction of the capacity for lipped channels. The positive imperfection makes the flanges of the lipped channel cross-section move outward at the mid-height, which provides lower post-buckling strength (Dinis, Camotim, & Silvestre, 2007). Accordingly, the PGPDPL imperfection pattern is adopted as a lower-bound assumption for performing parametric analyses. The positive sign for the global imperfection (bow and camber) is always defined to insure that the eccentricities are maximum at the mid-height of the specimen. The selected shapes of the imperfections are schematically shown in Figure 4. The 50% CDF values are used for the imperfection magnitude (Torabian et al., 2014a; Zeinoddini & Schafer, 2012). These assumptions on the imperfection result in a biased model (conservatively) for the strength prediction (at least -3%), which can be considered in the interpretation of the results.

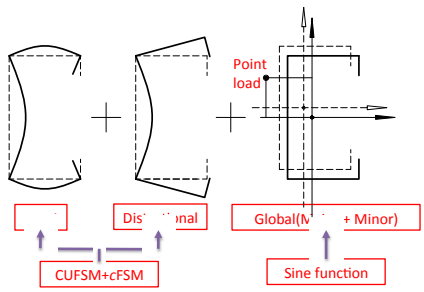

Figure 4 Imperfections pattern (positive sign convention) used in the parametric study

Loading and solution method

Including one specimen for pure axial loading, 127 evenly distributed P-M_1-M_2 load combinations (30^o intervals in azimuth and 5^o in elevation direction) are considered for each beam-column model. Displacement is applied at the reference node (see Figure 3b) for most of the specimens except for the specimens that has large eccentricity (more like a beam). For those specimens, force and moment are applied at the reference node. In the parametric study, the arc-length (Riks) method is implemented for the equilibrium solver.

Parametric analysis matrix: Cross-section selection

There are 364 structural stud cross-sections in the SFIA product list for structural lipped channels (SFIA, 2012). Depths of the cross-sections vary from 2.5 to 16 inches. To select a representative subset, several dimensionless parameters are considered to characterize the cross-sections in the product list. Accordingly, 75 cross-sections covering the range of variations of the selected dimensionless parameters are employed in the parametric analyses.

The dimensionless parameters considered are depth-to-width ratio (Figure 5a), flange-to-lip ratio (Figure 5b), local (Figure 5c) and distortional (Figure 5d) slenderness, and the ratio of local to distortional nominal axial capacity (Figure 5e and 5f). The popularity of the cross-sections in construction, and cross-sections used in previous experiments are also considered in selecting the final cross-sections for the parametric study.
Local (P_{crl}) and distortional (P_{crd}) axial buckling loads and the corresponding half-wave lengths, L_{crl} and L_{crd} are calculated using CUFSM 4.06. Assuming the

yield load for column global buckling, $P_{ne}=P_y$, the local (λ_l) and distortional (λ_d) slenderness are determined for all cross-sections.

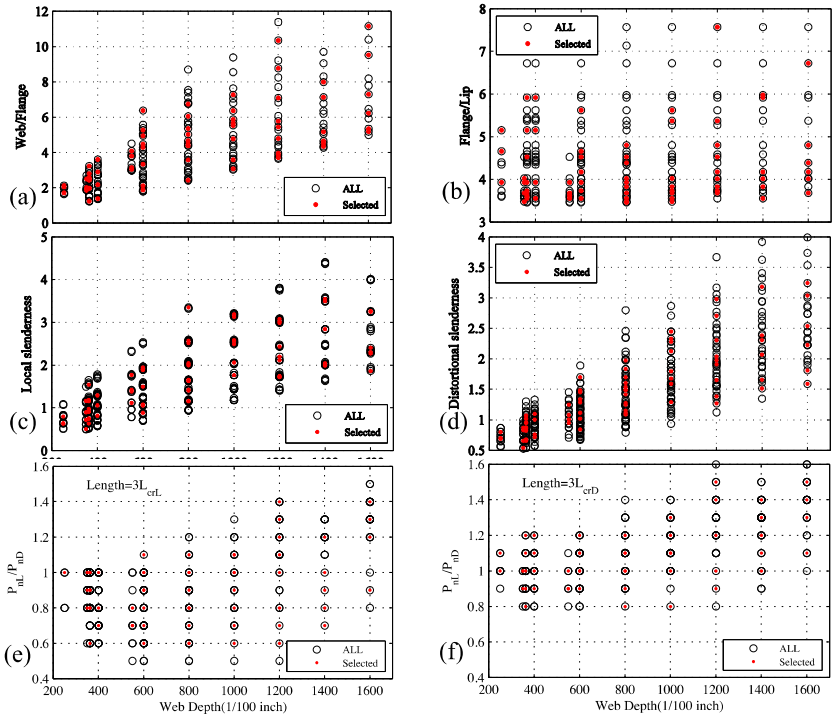

Figure 5 Selecting cross-sections for parametric study based on the dimension parameters

Using the calculated local and distortional slenderness, the axial nominal capacity of the cross section is also determined to identify the governing mode of failure of the specimens. To account for the clamped distortional buckling end condition, an empirical relationship developed for boosting the distortional buckling critical load is implemented to the elastic distortional buckling load and the associated distortional slenderness (Moen, 2008; Torabian et al., 2014a). A length of $3L_{crl}$ is assumed for short specimens which provides a large increase above the simply supported distortional buckling minimum, and a length of $3L_{crd}$ is assumed for longer specimens which provides minimal increase to the simply supported elastic distortional buckling load. The axial capacity of the specimens having both lengths is calculated for all cross-sections. The P_{crl}/P_{crd} ratio is used to identify whether the local or the distortional buckling governs the specimen strength. As a summary, the parametric analysis matrix is consisted of 75 cross-

sections, 2 different lengths ($3L_{crl}$ and $3L_{crd}$) and 127 load combinations for each model. Accordingly, 19,050 different beam-column models have been analyzed to failure to evaluate the prediction methods.

FEM results and reliability analysis

To study the results more quantitatively, the reliability index or safety index, β_0, which is a measure of the reliablity or safety of the structural member, is determined based on the available parametric study results and the corresponding predicted results. Pridiction methods include current AISI-S100-12 (DSM method) and the proposed beam-column DSM presented herein. These two methods share common anchor points for isolated P, M_1 and/or M_2. Larger β_0 implies higher reliability and lower probabilty of failure.. The reliability index is calculated using the method described in Chapter F of AISI-S100 (2012) (AISI-S100, 2012). Correspondingly, the strength of the tested member should satisfy Eq. F1.1-1a of AISI-S100 (for LRFD) as follows (AISI-S100, 2012),

$$\sum \gamma_i Q_i \le \phi R_n \tag{25}$$

where $\sum \gamma_i Q_i$ is the required strength (factored loads) based on the most critical load combination determined in accordance with Section A5.1.2 for LRFD; ϕ is the resistance factor and R_n is the average value of all test results. The resistance factor ϕ can be calculated as follows (AISI-S100, 2012),

$$\phi = C_\phi (M_m F_m P_m) e^{-\beta_0 \sqrt{V_m^2 + V_F^2 + C_P V_P^2 + V_Q^2}} \tag{26}$$

where, $C\phi$, the calibration factor is 1.52 for LRFD method (see more details in Meimand and Schafer, 2014); M_m is the mean material factor (M_m = 1.05); F_m is the mean fabrication factor (F_m = 1.00); P_m is the mean value of the professional factor (P_m is the mean of the test-to-predicted ratio); β_0 is the target reliability index which is assumed to be 2.5 for structural members (LRFD); V_m is the coefficient of variation for the material factor (V_m = 0.10); V_F is the coefficient of variation for the fabrication factor (V_F = 0.05); C_p=*(1+1/n)/m/(m-2)* is the correction factor, where n in the number of the tests (simulations) and m is the degrees of freedom (=*n-1*), since a large number of simulations have been done, C_P is assumed to be 1.0; V_P is the coefficient of variation for the professional factor (V_p is the coefficient of variation of the test-to-predicted ratio); V_Q is the coefficient of variation for the load effect (V_Q=0.21 for the LRFD method).

Mean test-to-predicted ratios (i.e., FEM-to-predicted ratio in this study) and the associated standard deviations for both current AISI-S100-12 (DSM method) and the proposed beam-column DSM are summerized in Table 1 for all specimens. Figure 6 illustrates the FEM-to-predicted ratio (β_{FEM}/β_n) scatter vs.

local slenderness for short specimens and vs. distortional slenderness for long specimens.

In Table 1a and 1b, the reliability index is back calculated from Eq. 5.2 for two different resistance factors; and the resistance factor is also calculated based on the target reliability of 2.5. Two resistance factors 0.85 (typical for columns) and 0.9 (typical for beams) have been investigated for the beam-column member.

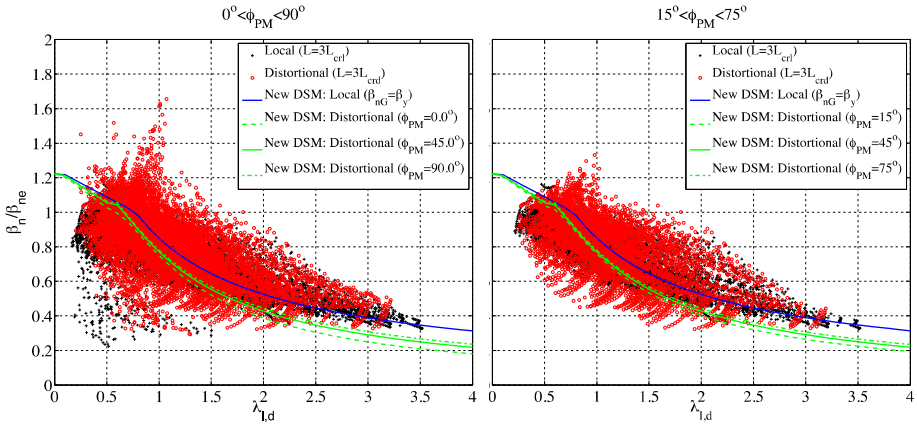

Figure 6 Results of the parametric study: (a) All points; (b) non-anchor points

As the anchor points are common between the proposed method and the current AISI-S100-12 method, evaluation at the anchor points provides the same reliability. Accordingly, in Table 1 two data sets are considered: Data set "All" that includes all data points (anchor and non-anchor points, see Figure 6a) and data set "15°<ϕ□□<75°" that includes just results away from the anchor points (Figure 6b). Although the difference is small, the non-anchor results provide a more reasonable reliability assessment for the newly proposed method.

The reliability analysis in Table 1a shows that the current beam-column design method in AISI-S100-12 is conservative. The calculated reliability indices of the AISI-S100-12 linear interaction equation for "15° <ϕ□□<75°" are 3.17 (ϕ=0.85) and 2.96 (ϕ=0.90), which are larger than the target reliability index of 2.5. The calculated reliability index of the newly proposed beam-column DSM method is 2.47 (ϕ=0.85) and 2.27 (ϕ=0.90); close to the target reliability index. As discussed previously, the modeling protocols used for simulation are a minimum of -5% biased in strength. Revising the mean values by 5% increase and recalculating the reliability indexes results in the reliability index of 2.64

(ϕ=0.85) and 2.44 (ϕ=0.90) for the newly proposed beam-column DSM method (Table 1b), which satisfies the target reliability index.

Table 1 Reliability analysis on design methods : (a) AISI-S100-12; (b) New DSM beam-column

(a)		AISI-S100-12 Linear Interaction				
	No. of spec.			β_0		ϕ
Data Set		P_m	V_p	ϕ=0.85	ϕ=0.9	β_0=2.5
All	19050	1.27	0.17	2.99	2.80	0.98
$15^o<\phi_{PM}<75^o$	13650	1.31	0.14	3.28	3.07	1.05

(b)		New Beam-Column DSM				
	No. of spec.			β_0		ϕ
Data Set		P_m	V_p	ϕ=0.85	ϕ=0.9	β_0=2.5
All	19050	1.08	0.18	2.39	2.20	0.82
$15^o<\phi_{PM}<75^o$	13650	1.08	0.16	2.47	2.27	0.84
$15^o<\phi_{PM}<75^o$ *	13650	1.14	0.16	2.64	2.44	0.88

* 5% increase in P_m due to biased modeling assumptions

Future Work

Work on an additional 36 Zee-section tests, refining and extending the parametric studies with the FE model, finalizing the design equations, and user-friendly computational design tools are ongoing.

Conclusions

A new design formulation that directly incorporates stability under the actual applied P-M_1-M_2 action and inelastic reserve in bending is proposed. This new Direct Strength Method (DSM) for beam-columns provides capacity predictions on average 20% higher than current design formulations, but still remains conservative - future improvements are also still desired. A comprehensive parametric analysis on lipped channels using a verified modeling protocol has been performed to evaluate the current beam-column design method and the proposed beam-column DSM. The parametric analysis includes 19,050 capacity points for 75 independent beam-column members. Reliability analyses of the current beam-column design method in the AISI specification and the newly proposed beam-column DSM using both test results and parametric analyses results show that the current method is a conservative design method and the new proposed method can provide a more reasonable strength prediction.

Acknowledgments

The authors would like to acknowledge the American Iron and Steel Institute (AISI) and the Metal Building Manufacturers Association (MBMA) for funding this study. Also, the Chinese Scholarship Council provided funding that made Baofeng Zheng's participation possible. Any opinions, findings, and conclusions or recommendations expressed in this material are those of the authors and do not necessarily reflect the views of the sponsors or other participants.

References

Dinis, P. B., Camotim, D., & Silvestre, N. (2007). FEM-based analysis of the local-plate/distortional mode interaction in cold-formed steel lipped channel columns. *Computers & Structures*, *85*(19-20), 1461–1474.

Hancock, G. (2003). Cold-formed steel structures. *Journal of Constructional Steel Research*, *59*(4), 473–487.

Kalyanaraman, V., & Jayabalan, P. (1994). Local buckling of stiffened and unstiffened elements under nonuniform compression. In *Twelfth International Specialty Conference on Cold-Formed Steel Structures*.

Li, Z., & Schafer, B. W. (2010). Application of the finite strip method in cold-formed steel member design. *Journal of Constructional Steel Research*, *66*(8-9), 971–980.

Loh, T. S. (1985). *Combined axial load and bending in cold-formed steel members.* Cornell University.

Macdonald, M., Heiyantuduwa, M. a., & Rhodes, J. (2008). Recent developments in the design of cold-formed steel members and structures. *Thin-Walled Structures*, *46*(7-9), 1047–1053.

Meimand, V. Z., & Schafer, B. W. (2014). Impact of load combinations on structural reliability determined from testing cold-formed steel components. *Structural Safety*, *48*, 25–32.

Miller, T. H., & Pekoz, T. (1994). Load-Eccentricity effects on cold-formed steel lipped-channel columns. *Journal of Structural Engineering*, *120*(3), 805–823.

Moen, C. D. (2008). *Direct strength design for cold-formed steel members with perforations*. Johns Hopkins University.

AISI-S100. (2012). *North American Specification for the design of cold-formed steel structural members*. Washington (DC, USA).

Pekoz, T. (1986). Developement of a unified approach to the design of cold-formed steel members. In *Eighth International Specialty Conference on Cold-Formed Steel Structures* (pp. 77–84). St. Louis, MO.

Peterman, K. D. (2012). *Experiments on the stability of sheated cold-formed steel studs under axial load and bending*. Johns Hopkins University.

Rondal, J. (2000). Cold formed steel members and structures: General Report. *Journal of Constructional Steel Research*, *55*, 155–158.

Schafer, B. W. (2008). Review: The Direct Strength Method of cold-formed steel member design. *Journal of Constructional Steel Research*, *64*(7-8), 766–778.

Schafer, B. W., & Adany, S. (2006). Buckling analysis of cold-formed steel members using CUFSM: Conventional and Constrained Finite Strip Methods. In *Eighteenth international specialty conference on cold-formed steel structure: University of Missouri-Rolla, Rolla, MO, United States*. Orlando, FL, United States.

SFIA. (2012). *Technical Guide for Cold-Formed Steel Framing Products*. Falls Church, VA, US: Steel Framing Industry Association.

Shifferaw, Y. (2010). *Section capacity of cold-formed steel members by the Direct Strength Method*. Johns Hopkins University.

Standards Australia. (2005). *Cold-formed steel structures: NZS 4600*. Sydney, Australia: Standards Australia.

Torabian, S., Zheng, B., & Schafer, B. W. (2014a). *Direct Strength Prediction of Cold-Formed Steel Beam-Columns*. Thin-walled Structures Group at The Johns Hopkins University. American Iron and Steel Institute (AISI).

Torabian, S., Zheng, B., & Schafer, B. W. (2014b). Experimental study and modeling of cold-formed steel lipped channel stub beam-columns. In *Proceedings of the Annual Stability Conference Structural Stability Research Council*. Toronto, Canada: SSRC.

Yiu, F., & Pekoz, T. (2000). Design of Cold-Formed Steel Plain Channels. In *Fifteenth International Specialty Conference on Cold-Formed Steel Structures* (pp. 13–22). St. Louis, MO.

Young, B. (2008). Research on cold-formed steel columns. *Thin-Walled Structures*, *46*(7-9), 731–740.

Zeinoddini, V. M., & Schafer, B. W. (2012). Simulation of geometric imperfections in cold-formed steel members using spectral representation approach. *Thin-Walled Structures*, *60*, 105–117.